

1 **Weathering and persistence of plastic in the marine**  
2 **environment: Lessons from LEGO**

3

4 **Andrew Turner\*<sup>1</sup>, Rob Arnold<sup>2</sup>, Tracey Williams<sup>3</sup>**

5 <sup>1</sup>School of Geography, Earth and Environmental Sciences,

6 University of Plymouth

7 Drake Circus

8 Plymouth PL4 8AA, UK

9 aturner@plymouth.ac.uk

10

11 <sup>2</sup>Rame Peninsula Beach Care

12 56 Fore Street

13 Kingsand

14 Torpoint PL10 1NA, UK

15

16 <sup>3</sup>The Lego Lost At Sea Project

17 Old Bridge House

18 Porth Bean Road

19 Newquay TR7 3LU, UK

20

21 **Accepted 28<sup>th</sup> February 2020**

22 **[doi.org/10.1016/j.envpol.2020.114299](https://doi.org/10.1016/j.envpol.2020.114299)**

23

24 **Abstract**

25 The residence times of plastics in the oceans are unknown, largely because of the durability of the  
26 material and the relatively short (decadal) period of time over which plastic products have been  
27 manufactured. In this study, classic LEGO bricks constructed of acrylonitrile butadiene styrene (ABS)  
28 and washed up on the strandlines of beaches of southwest England have been subjected to X-ray  
29 fluorescence (XRF) analysis and the spectra and any other identifiers matched with unweathered  
30 blocks stored in collections or sets of known history. Relative to unweathered equivalents,  
31 weathered blocks exhibit varying degrees of yellowing, fracturing and fouling, and are of lower mass,  
32 average stud height and mechanical strength. These effects are attributed to photo-oxidative  
33 degradation and the actions of physical stress and abrasion while exposed to the marine  
34 environment. Infrared spectra indicate that the polymer remains largely intact on weathering but  
35 with photo-degradation of the polybutadiene phase of ABS, while quantification of XRF spectra  
36 reveals that pigments like cadmium sulphoselenide become more heterogeneously distributed in the  
37 matrix when in the environment. Using measured mass loss of paired (weathered versus  
38 unweathered) equivalents and the age of blocks obtained from storage we estimate residence times  
39 of between about 100 and 1300 years for this type and thickness of plastic, with variations reflecting  
40 differences in precise additive composition and modes of weathering.

41

42 **Capsule:** The weathering and persistence of plastic at sea has been studied by comparing LEGO  
43 blocks washed up on beaches with archived LEGO blocks of a similar age.

44

45 **Keywords:** LEGO; plastic; acrylonitrile butadiene styrene; marine; weathering; residence times

46

47 **1. Introduction**

48 Marine plastic has a variety of well-established impacts in the environment and on wildlife (Sheavy  
49 and Register, 2007; Barnes et al., 2009; Wilcox et al., 2016). Many of these impacts are highly  
50 pervasive and result from the exceptional durability of the material, or the very properties that make  
51 it such a versatile and widely-used commodity. Although plastic in the ocean is persistent, it will  
52 slowly weather through photo-oxidative degradation of the polymer and physical stress on the  
53 material (by, for example, abrasion and impaction). Markers of abiotic plastic degradation include a  
54 reduction in average molecular weight of the polymer, loss of mechanical properties, changes in

55 surface characteristics (e.g. colour, texture) and shifts in spectral signatures (Andrady, 2015), with  
56 the latter characteristic forming the basis of most mechanistic and quantitative studies (Cooper and  
57 Corcoran, 2010; Turner and Holmes, 2011; Zhu et al., 2019).

58 The precise rates of plastic weathering in the marine environment are difficult to ascertain because  
59 the material has only been manufactured over a relatively short (decadal) time period and the  
60 original compositions and properties of polymers vary considerably (Ter Halle et al., 2017).  
61 Moreover, empirical studies conducted in the laboratory or field, where material is exposed to  
62 natural or simulated sunlight, and with or without abrasive particulates, have been restricted to  
63 timeframes of a few weeks to a few years (Da Costa et al., 2018; Brandon et al., 2016; Biber et al.,  
64 2019). An alternative, indirect means of studying plastic weathering and persistence and estimating  
65 age of deposition over a longer period is to consider negatively buoyant items with a distinct  
66 temporal source. For example, Ioakeimidis et al. (2016) compared clear polyethylene terephthalate  
67 (PET) bottles trawled from the bed of the Saronikos Gulf, Greece, with a newly purchased PET bottle,  
68 and were able to relate shifts in spectral band intensities from Fourier Transform Infrared (FTIR)  
69 spectrometry with expiration dates spanning a period of nearly two decades. Assuming that  
70 expiration dates are a proxy for time of deposition, the authors concluded that PET remains intact  
71 for approximately fifteen years, whereafter there was a significant decrease in the occurrence of  
72 native functional groups indicating chemical changes.

73 Over the past decade, voluntary organisations from Cornwall, southwest England, have retrieved  
74 plastic waste from beach cleans throughout the county, with items of interest archived. Among  
75 these items are blocks of classic LEGO, identifiable from distinct studs and tubes and, in many cases,  
76 specific design numbers within the interior structure. Since 1966, European LEGO has been  
77 constructed of acrylonitrile butadiene styrene (ABS), an amorphous, thermoplastic copolymer made  
78 of an acrylonitrile–styrene continuous phase and partially grafted polybutadiene that acts as an  
79 impact modifier (Saviello et al., 2014). The density of ABS ranges from about 1 to 1.2 g cm<sup>-3</sup>  
80 depending on processing method, performance requirements (or relative abundance of the three  
81 monomers) and the type and amount of functional additives present (Mitchell, 1996). Regarding  
82 LEGO, additives have evolved over the years because of changes in material costs, production  
83 locations, technology and environmental regulations. Of particular significance in respect of the  
84 latter is the use of the now restricted brightly-coloured yellow and red cadmium-based pigments  
85 from the early 1970s to the early 1980s (Turner, 2018).

86 In the present study, samples of classic LEGO blocks temporarily washed up on the strandlines of  
87 beaches of southwest England have been matched with blocks in ~ 40+ year-old collections or sets

88 that have not undergone environmental exposure from similarities in their secondary (fluorescent)  
89 X-ray spectra. Weathered and unweathered sample pairs are quantitatively and qualitatively  
90 compared using a variety of techniques in order to examine the physical and chemical changes and  
91 rates of weathering effected by exposure to the marine environment over decadal timeframes.

92

## 93 **2. Materials and Methods**

94 About 50 beached LEGO blocks (bricks, plates, tiles) were supplied to the university from archived  
95 litter collections (dating back to 2010) held by various voluntary organisations engaged in regular  
96 beach cleans in Cornwall, the most southwesterly county in England that is bordered by the western  
97 English Channel to the south and the southern Celtic Sea to the north. In theory, blocks are denser  
98 than coastal sea water ( $\sim 1.02 \text{ g cm}^{-3}$ ) and should sink, but plastic of this nature appears to be  
99 beached in Cornwall under certain tidal and meteorological conditions. In particular, relatively dense  
100 plastics can be found amongst large deposits of kelp washed up after strong onshore winds and large  
101 swell.

102 In the laboratory, LEGO blocks were rinsed under tap water and as much visible adherent or trapped  
103 extraneous material as possible (mainly sand and grit) was removed with a Nylon brush or metal  
104 tweezers. Samples were air-dried at 40°C for an hour before being individually weighed on a five-  
105 figure Sartorius Genius balance; the length, width and height of each block and the height of all or at  
106 least three studs through their centres were then determined to  $\pm 10 \mu\text{m}$  with Allendale digital  
107 callipers. Density was estimated from the mass of tap water displaced by each block when  
108 suspended on a steel wire attached to the roof panel of the balance.

109 The chemical characteristics of each block were determined at between 4 and 12 locations by a  
110 battery-operated, energy-dispersive X-ray fluorescence (XRF) spectrometer (Niton XL3t He GOLDD+;  
111 Turner and Solman, 2016). The instrument was housed in an accessory stand with the nose pointing  
112 upwards, and the measurement surface was suspended just above the 8-mm diameter detector  
113 window. Counting was conducted in a plastics mode with a thickness correction of 1.5 mm (the  
114 approximate thickness of most blocks) for 20 seconds at 40  $\mu\text{A}$  and 50 kVp and 10 seconds at 100  $\mu\text{A}$   
115 and 20 kVp.

116 Blocks of the same (or original) colour, structure and size and, if available, serial number or internal  
117 signage, that had been boxed while not in use and that were in good condition (“unweathered”)  
118 were sourced from collections purchased in the UK between 1972 and 1981. Samples were  
119 subjected to XRF analysis as above and those whose spectra and pigment composition most closely

120 matched beached (“weathered”) blocks were paired. Particular attention was paid to compounds of  
121 Cd as these were employed over a specific timeframe that is difficult to define precisely but appears  
122 to have been from the early 1970s until their replacement on health and environmental grounds at  
123 the beginning of the following decade (Compound Interest, 2019). Specifically, high quantities of CdS  
124 and  $\text{CdS}_{1-x}\text{Se}_x$  ( $0 \leq x \leq 1$ ) were employed as bright yellow and red pigments, respectively, while  
125 unknown Cd compounds appear to have been added at lower concentrations to blocks of other  
126 colours but whose function is unclear (Turner, 2018). Examples of paired sample spectra are  
127 illustrated in Figure 1 for red bricks with common characteristic peaks for Cd, Se and Ba (sample 1)  
128 and for white bricks with common peaks for Ti but without Zn that was present in many other white  
129 LEGO blocks (sample 4). Unweathered samples were measured for mass, size, stud height and  
130 density as above and were retained for comparative purposes and further characterisation.

131 Weathered and unweathered LEGO blocks were analysed by attenuated total reflectance Fourier-  
132 transform-infrared (ATR-FTIR) spectrometry using a Bruker Vertex 70. A stainless steel scalpel was  
133 used to scrape a piece of a few mg from different regions of the sample surface to a depth of about  
134 100  $\mu\text{m}$ . Scrapings were clamped with the outer face against the diamond crystal before spectra  
135 were acquired with 16 scans in the region 4000 to 600  $\text{cm}^{-1}$  and at a resolution of 4  $\text{cm}^{-1}$ . The  
136 surfaces of selected weathered and unweathered blocks were photographed under a Nikon SMZ800  
137 stereo-microscope, while the surface morphology and surficial elemental composition of these  
138 blocks were compared by scanning electron microscopy (SEM) using a JEOL JSM-6610. The electron  
139 microscope was operated with an accelerating voltage of 15 kV and in a low vacuum mode, and was  
140 outfitted with an Oxford Instruments energy dispersive X-ray spectrometer (EDS) and Aztec  
141 software. The mechanical strength of selected weathered and unweathered blocks was determined  
142 in compression tests using an Instron 5582 Universal Tester operated at a crosshead speed of 2 mm  
143  $\text{min}^{-1}$  and with load-displacement data monitored and recorded in Merlin software.

144

### 145 **3. Results and Discussion**

#### 146 *3.1. Visual and physical changes of LEGO blocks on weathering*

147 The blocks subject to weathering in the marine environment that are considered in the study are  
148 shown in Figure 2 alongside corresponding unweathered blocks that were paired in terms of age and  
149 origin from similarities in XRF spectra. Thus, a total of 14 pairs were identified, with the majority  
150 comprising classic bricks of 2, 4 or 8 studs; remaining pairs consisted of a sloping (roof) brick (sample  
151 8), a brick with a moulded axel housing (sample 6), a 2-studded plate (sample 13) and a 1-studded

152 cylinder (sample 14). Weathered blocks have smoother edges and corners compared with  
153 unweathered equivalents, and their glossy sheen is lost and the embossed LEGO logo on the studs  
154 and any designed textures have disappeared. While the colour of black, grey and green blocks  
155 remain on weathering, red, yellow and blue blocks appear to fade or haze and all red blocks and one  
156 white block exhibit evidence of “yellowing”. Aside from smoothing and denudation, many  
157 weathered blocks reveal structural deformities, including distortion or contraction, and evidence of  
158 fracturing and fragmentation, with pits, grooves or gaps along the side or top face and missing  
159 connecting pins or cracked tubes in the interior. Overall, five weathered bricks were sufficiently  
160 fractured that significant parts of the structure (at least 3 mm in the longest dimension) were  
161 absent, and in two of these cases there were visible accumulations of biofouling, including  
162 calcareous deposits from what appeared to be the tube-building worm, *Spirobranchus triqueter*,  
163 within the internal structure.

164 Measurements of length, width and thickness did not vary systematically among paired samples and  
165 could not be used to evaluate the degree of block weathering; for example, in some cases measured  
166 dimensions increased upon weathering because of distortion of part or all of the plastic structure  
167 (compare, for example, block shapes in paired sample 7 in Figure 2). Height, however, and in  
168 particular stud height, appeared to provide a more robust evaluation of the extent of sample  
169 weathering as and shown in Table 1. Here, the mean height of studs on unweathered blocks ranges  
170 from about 1.7 to 1.9 mm while on weathered blocks mean height ranges from 0.5 to 1.8 mm, and in  
171 all but one case where multiple measurements were taken there is a statistically significant  
172 reduction in stud height ( $p < 0.05$ ) on weathering according to a series of two-sample *t*-tests. Overall,  
173 stud height is reduced significantly by between about 8% and over 60% on block weathering.

174 Also shown in Table 1 are the masses of unweathered and weathered sample pairs. Here,  
175 unweathered mass is given as a single value but where replicate matching blocks were available  
176 mass varied by less than 1%. Mass reduction on weathering ranges from about 3% to 40% but this  
177 measure did not correlate with stud height reduction because the greatest losses in mass were  
178 accompanied by absence (through fracturing-disintegration) of significant parts of the LEGO block  
179 structure itself. Moreover, in some cases mass reduction was partially offset by visible fouling or  
180 entrapment of particulates that could not be shifted on cleaning.

181 All but three unweathered blocks sank in tap water and estimates of density derived from water  
182 mass displacement ranged from 1.00 to 1.17 g cm<sup>-3</sup>. Overall, however, there were no clear density  
183 differences between weathered and unweathered blocks, with colour, and presumably additive

184 composition, having a more important effect on the results (grey and white blocks were densest and  
185 green and black blocks least dense).

186 Results of the compression tests are exemplified for two sample pairs in Figure 3. Here, the left and  
187 right peaks in the load-displacement distributions are associated with the compression of studs into  
188 the top wall and yielding of the block, respectively, with the maximum load in the latter peak  
189 indicative of ultimate compressive strength. Subsequent irregularities in the distributions, that are  
190 particularly apparent in weathered block 3, are indicative of multiple failures taking place. Overall,  
191 we may conclude that weathered blocks are mechanically weaker and more brittle than their  
192 unweathered counterparts.

193

### 194 *3.2. Microscopy and chemical effects*

195 Microscopic images of the studded areas of two sample pairs, shown in Figure 4, illustrate the scale  
196 and heterogeneity of the aforementioned effects of weathering on the LEGO surface more clearly. In  
197 addition, comparative images reveal the extent of white bio-deposits on the surface of some  
198 weathered blocks and the propensity for cracks and pits to trap grains of sand and other microscopic  
199 debris. Images of greater magnification derived from SEM are exemplified for sample pair 10 in  
200 Figure 5. For the unweathered brick, the surface is relatively flat and uniform, and EDS results  
201 probing the upper few tens of microns of the sample are consistent with the composition of the  
202 polymeric matrix and the presence of (i) oxygen as oxidised products or as a component of inorganic  
203 additives, (ii) a Ba-based additive (that appears to be restricted to the light-coloured areas) and (iii)  
204 the bright yellow pigment, cadmium sulphide. The weathered brick is more heterogeneous in  
205 appearance, with microscopic cracks, notches, pores, pits and grooves distributed across the surface,  
206 and the EDS results indicate the presence of residual seawater salts and both inorganic (e.g. Al, Fe)  
207 and biological (e.g. Ca, Si) fouling that obscure the chemical characteristics of the underlying plastic.

208 A more accurate but less sensitive evaluation of the concentration of a smaller range of elements in  
209 the samples was obtained by XRF spectrometry that employs a higher energy X-ray beam.

210 Specifically, concentrations averaged through the 1.5 mm thickness of ABS were acquired from  
211 fluorescent spectral peaks that had been subject to fundamental parameters calculations using  
212 Niton NDT software. In individual unweathered blocks, and where detected, the XRF returned similar  
213 concentrations of Ba, Cd, Se, Ti and Zn over each surface, including studded areas, suggesting an  
214 homogenous distribution of pigments and other inorganic additives throughout the ABS, and that  
215 surface geometry does not exert a measurable impact on the results. For weathered blocks,

216 elemental concentrations were more varied across each sample suggesting a heterogeneous  
217 dissociation and migration of additives from the plastic as well as variable rates of disintegration of  
218 the plastic matrix. This effect is exemplified in Figure 6 for concentrations of Se versus  
219 concentrations of Cd determined over multiple areas of the surface ( $n = 4$  to 12) of three sample  
220 pairs where cadmium sulphoselenide was used for colour. Thus, individual weathered blocks exhibit  
221 a wider distribution of concentrations of Se or Cd (or both Se and Cd) than corresponding  
222 concentrations returned for unweathered blocks, and the effect is most pronounced for paired  
223 sample 1 where the weathered brick exhibited considerable distortion, fracturing and fouling. Note  
224 that the gradient of the mass relationship defining Se and Cd in unweathered blocks (0.155) suggests  
225 that the structure of the original pigment in the ABS may be approximated as:  $\text{CdS}_{0.78}\text{Se}_{0.22}$ .

226 FTIR spectra of weathered and unweathered LEGO blocks are exemplified in Figure 7 for four sample  
227 pairs of different colours. The majority of main bands in both spectra are consistent with the  
228 principal absorbing groups of ABS (e.g. styrene, acrylonitrile and butadiene; Saviello et al., 2014),  
229 with spectral intensities similar in all cases with the exception of black bricks where infrared  
230 radiation is readily absorbed (Becker et al., 2017). Overall, therefore, there is no clear evidence of  
231 the presence of organic additives in the matrix and it appears that the polymer remains largely intact  
232 on weathering, possibly because of the protective effects afforded by fouling, certain oxidation  
233 products or coloured pigments (Iannuzzi et al., 2013). The most significant differences between  
234 weathered and unweathered blocks appear to be restricted to the accentuation of a peak at 1735  
235  $\text{cm}^{-1}$  and the appearance of a peak at 1270  $\text{cm}^{-1}$  on weathering. The former is due to carbonyl  
236 stretching of an ester group formed by the photo-oxidation of the polybutadiene phase of ABS while  
237 the latter likely results from C-O stretching in oxidation products containing, for example, carboxylic  
238 acids (Saviello et al., 2014).

239

### 240 *3.3. Rates and mechanisms of LEGO weathering*

241 Because weathered LEGO blocks washed up on and retrieved from beaches of southwest England  
242 over the past decade were successfully paired with unweathered equivalents that were  
243 manufactured and purchased between the early 1970s and early 1980s, we may surmise that  
244 beached samples have been exposed to the local marine environment for between 30 and 40 years.  
245 Precisely how these blocks entered the environment, however, is unclear. In 1997 a well-  
246 documented spillage of specific sets of customised LEGO pieces occurred off the coast of south west  
247 England (Osgood and Robinson, 2019) but no earlier spillages have been reported in the media or  
248 literature and the samples studied here do not appear to belong to specific sets. It is possible that



249 individual blocks are lost at play on the beach but research and calculations undertaken by one of  
250 the UK's largest insurance companies suggests that over two million blocks have been flushed down  
251 the toilet by children under ten years old (Direct Line Home Insurance, 2016). Depending on the  
252 presence, nature and performance of historical waste water treatment plants, an unknown  
253 proportion of blocks lost during the early 1970s to early 1980s will have entered the aquatic  
254 environment via this route.

255 In theory, LEGO ABS is inherently denser than seawater, suggesting that blocks have a propensity to  
256 sink in the marine environment. This was confirmed by the density measurements of all weathered  
257 and most unweathered blocks being above  $1.03 \text{ g cm}^{-3}$ . There is, however, no means of ascertaining  
258 precisely how and where the LEGO blocks were weathered. For example, blocks may have been  
259 gradually degraded photolytically in seawater during suspension above or deposition on the seabed,  
260 an effect that is often constrained by the protective (e.g. shading) properties of surface fouling  
261 (Andrady, 2015); abrasive weathering by sediment and other particulates may have taken place  
262 during turbulence near or on the seabed (and particularly in the swash zone), and fracturing may  
263 have resulted from physical stress and impaction on hard surfaces. It is also significant that Cd  
264 sulphide and sulphoselenide pigments are light-sensitive (Fowles, 1977; Liu et al., 2017) because we  
265 may surmise that pigment release as well as polymer breakdown are accelerated in the photic zone.  
266 This assertion is consistent with the presence of visible calcareous biodeposits on the most  
267 weathered red and yellow cadmium-pigmented blocks.

268 Regardless of the precise mechanisms of LEGO block weathering, an evaluation of environmental  
269 persistence may be gained from the mass losses reported in Table 1 and the aforementioned  
270 estimates of periods of exposure. Thus, neglecting any fouling and accumulation of material, net  
271 block mass loss ranges from about 3% to 40%, suggesting that this type and thickness of plastic may  
272 remain in the marine environment for between about 100 and 1300 years. Presumably, upper  
273 estimates reflect gradual degradation, possibly where light is limited, and lower estimates involve  
274 additional physical stress and subsequent fragmentation. These estimates compare with life  
275 expectancies of clear polyethylene terephthalate bottles (whose thickness is typically a few hundred  
276  $\mu\text{m}$ ) of between several tens and one hundred years (Ioakeimidis et al., 2016) and are consistent  
277 with the assertion that the residence times of plastics in the ocean are believed to exceed the  
278 timeframes over which the materials have been manufactured (Barnes et al., 2009).

279

#### 280 **4. Conclusions**

281 In summary, analysis of paired weathered-unweathered LEGO blocks has allowed the physical and  
282 chemical effects of marine environmental exposure on pigmented ABS plastic to be examined.  
283 Weathering over decadal timeframes results in smoothing, discolouration and fouling of the plastic  
284 surface and deformation, fracturing and fragmentation of the structure, with leaching of additives  
285 and pigments from the matrix proceeding at variable rates. Based on mass difference among paired  
286 samples that are about 40 years old we estimate residence times in the marine environment on the  
287 order of hundreds of years.

288

## 289 **Acknowledgements**

290 The authors are grateful for the technical support provided by Mr Billy Simmonds and Mr Glenn  
291 Harper, Plymouth University. The study was funded partly by a Plymouth Marine Institute HEIF  
292 Award.

293

## 294 **References**

- 295 Andrady, A.L., 2015. Persistence of plastic litter in the oceans. In: *Marine Anthropogenic Litter*, ed.  
296 M. Bergmann, L. Gutlow, M. Klages. Springer, pp. 57-72.
- 297 Barnes, D.K.A., Galgani, F., Thompson, R.C., Barlaz, M., 2009. Accumulation and fragmentation of  
298 plastic debris in global environments. *Philosophical Transaction of the Royal Society of London: B*  
299 *Biological Sciences* 364, 1985-1998.
- 300 Becker, W., Sachsenheimer, K., Klemenz, M., 2017. Detection of black plastics in the middle infrared  
301 spectrum (MIR) using photon up-conversion technique for polymer recycling purposes. *Polymers* 9,  
302 435 doi:10.3390/polym9090435
- 303 Biber, N.F.A., Foggo, A., Thompson, R.C., 2019. Characterising the deterioration of different plastics  
304 in air and seawater. *Marine Pollution Bulletin* 141, 595-602.
- 305 Brandon, J., Goldstein, M., Ohman, M.D., 2016. Long-term aging and degradation of microplastic  
306 particles: Comparing in situ oceanic and experimental weathering patterns. *Marine Pollution Bulletin*  
307 110, 299-308.
- 308 Compound Interest, 2019. What are LEGO bricks made of?  
309 <https://www.compoundchem.com/2018/04/09/lego/> accessed 8/19
- 310 Cooper, D.A., Corcoran, P.L., 2010. Effects of mechanical and chemical processes on the degradation  
311 of plastic beach debris on the island of Kauai, Hawaii. *Marine Pollution Bulletin* 60, 650-654.
- 312 Da Costa, J.P., Nunes, A.R., Santos, P.S.M., Girao, A.V., Duarte, A.C., Rocha-Santos, T., 2018.  
313 Degradation of polyethylene microplastics in seawater: Insights into the environmental degradation  
314 of polymers. *Journal of Environmental Science and Health Part A: Toxic/Hazardous Substances and*  
315 *Environmental Engineering* 53, 866-875.

316 Direct Line Home Insurance, 2016. [https://www.directline.com/media/archive-2016/millions-of-  
317 Lego-bricks-get-flushed-down-the-toilet](https://www.directline.com/media/archive-2016/millions-of-317 Lego-bricks-get-flushed-down-the-toilet) accessed 8/19.

318 Fowles, G.W.A., 1977. The leaching of cadmium from plastic toys. *Science of the Total Environment*  
319 7, 207-216.

320 Iannuzzi, G., Mattsson, B., Rigdahl, M., 2013. Color changes due to thermal ageing and artificial  
321 weathering of pigmented and textured ABS. *Polymer Engineering and Science* DOI  
322 10.1002/pen.23438.

323 Ioakeimidis, C., Fotopoulou, K.N., Karapanagioti, H.K., Geraga, M., Zeri, C., Papathanassiou, E.,  
324 Galgani, F., Papatheodorou, G., 2016. The degradation potential of PET bottles in the marine  
325 environment: An ATR-FTIR based approach. *Scientific Reports* 6:23501 DOI: 10.1038/srep23501.

326 Liu, H., Gao, H., Long, M., Fu, H., Alvarez, P.J.J., Li, Q., Zheng, S., Qu, X., Zhu, D., 2017. Sunlight  
327 promotes fast release of hazardous cadmium from widely-used commercial cadmium pigments.  
328 *Environmental Science and Technology* 51, 6877-6886.

329 Mitchell, P.E., 1996. *Tool and Manufacturing Engineers Handbook*, fourth edition. Vol. VIII: Plastic  
330 Part Manufacturing. Society of Manufacturing Engineers, Dearborn, Michigan.

331 Osgood, J., Robinson, K.H., (editors) 2019. *Feminists Researching Gendered Childhoods: Generative*  
332 *Entanglements*. Bloomsbury Press 192pp.

333 Saviello, D., Pouyet, E., Toniolo, L., Cotte, M., Nevin, A., 2014. Synchrotron-based FTIR  
334 microspectroscopy for the mapping of photo-oxidation and additives in acrylonitrile–butadiene–  
335 styrene model samples and historical objects. *Analytica Chimica Acta* 843, 59-72.

336 Sheavy, S.B., Register, K.M., 2007. Marine debris and plastics: Environmental concerns, sources,  
337 impacts and solutions. *Journal of Polymers and the Environment* 15, 301-305.

338 Ter Halle, A., Ladriat, L., Martignac, M., Mingotaud, A.F., Boyron, O., Perez, E., 2017. To what extent  
339 are microplastics from the open ocean weathered? *Environmental Pollution* 227, 167-174.

340 Turner, 2018. Concentrations and migratabilities of hazardous elements in second-hand children’s  
341 plastic toys. *Environmental Science and Technology* 52, 3110-3116.

342 Turner, A., Holmes, L., 2011. Occurrence, distribution and characteristics of beached plastic  
343 production pellets on the island of Malta (central Mediterranean). *Marine Pollution Bulletin* 62, 377-  
344 381.

345 Turner, A., Solman, K.R., 2016. Analysis of the elemental composition of marine litter by field-  
346 portable-XRF. *Talanta* 159, 262-271.

347 Wilcox, C., Mallos, N.J., Leonard, G.H., Rodriguez, A., Hardesty, B.D., 2016. Using expert elicitation to  
348 estimate the impacts of plastic pollution on marine wildlife. *Marine Policy* 65, 107-114.

349 Zhu, K.C., Jia, H.Z., Zhao, S., Xia, T.J., Guo, X.T., Wang, T.C., Zhu, L.Y., 2019. Formation of  
350 environmentally persistent free radicals on microplastic under light irradiation. *Environmental*  
351 *Science and Technology* 53, 8177-8186.

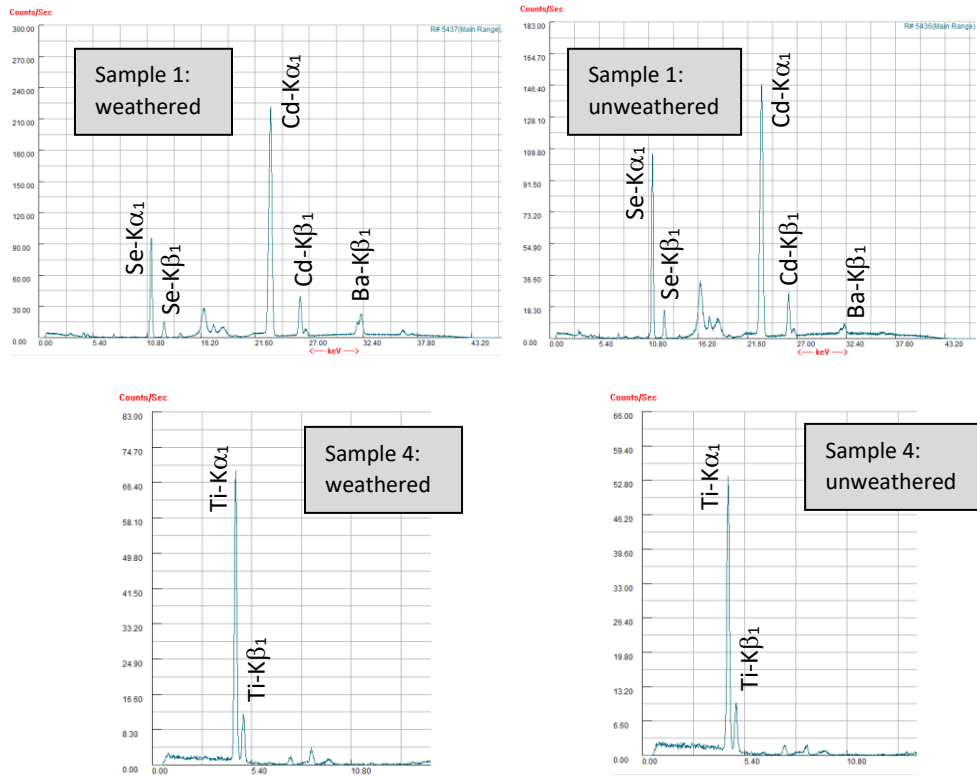
352 Table 1: Mean stud height ( $\pm$  one standard deviation) and mass for weathered and unweathered pairs of LEGO blocks, and the mean percentage reduction  
 353 of stud height and mass on weathering. Asterisks denote a significant reduction in stud height on weathering according to a series of two-sample *t*-tests.

sample pair	weathered		unweathered		reduction on weathering	
	stud height, mm	mass, g	stud height, mm	mass, g	stud height, %	mass, %
1	1.13 $\pm$ 0.10	2.429	1.78 $\pm$ 0.07	3.248	36.2*	25.2
2	1.49 $\pm$ 0.09	2.091	1.71 $\pm$ 0.02	2.216	13.1*	5.66
3	1.11 $\pm$ 0.29	1.750	1.80 $\pm$ 0.03	2.179	38.4*	19.7
4	1.64 $\pm$ 0.05	1.347	1.79 $\pm$ 0.06	1.467	8.40*	8.20
5	1.67 $\pm$ 0.10	0.639	1.72 $\pm$ 0.10	0.831	2.91	23.1
6	1.24 $\pm$ 0.50	1.229	1.84 $\pm$ 0.05	1.358	32.7*	9.40
7	1.29 $\pm$ 0.45	1.139	1.92 $\pm$ 0.05	1.370	32.5*	16.9
8	0.66 $\pm$ 0.61	1.250	1.94 $\pm$ 0.05	2.079	66.3*	39.8
9	1.11 $\pm$ 0.17	0.908	1.74 $\pm$ 0.07	1.366	36.3*	31.6
10	1.02 $\pm$ 0.16	2.356	1.72 $\pm$ 0.03	2.598	40.6*	9.31
11	1.31 $\pm$ 0.02	1.465	1.78 $\pm$ 0.04	2.175	26.2*	32.6
12	0.54 $\pm$ 0.16	1.034	1.69 $\pm$ 0.07	1.395	67.9*	25.8
13	1.54 $\pm$ 0.06	0.349	1.88 $\pm$ 0.04	0.363	18.4*	3.91
14	1.74	0.304	1.89	0.313	7.94	2.88
median	1.27	1.2395	1.79	1.431	32.6	18.3

354

355 Figure 1: Examples of spectra used to pair the weathered and unweathered blocks shown in Figure  
356 2.

357  
358



359 Figure 2: Weathered and unweathered blocks paired from appearance, signage and similarities in  
360 XRF spectra and shown on cm-scaled graph paper.

361

362

363

364

365

366

367

368

369

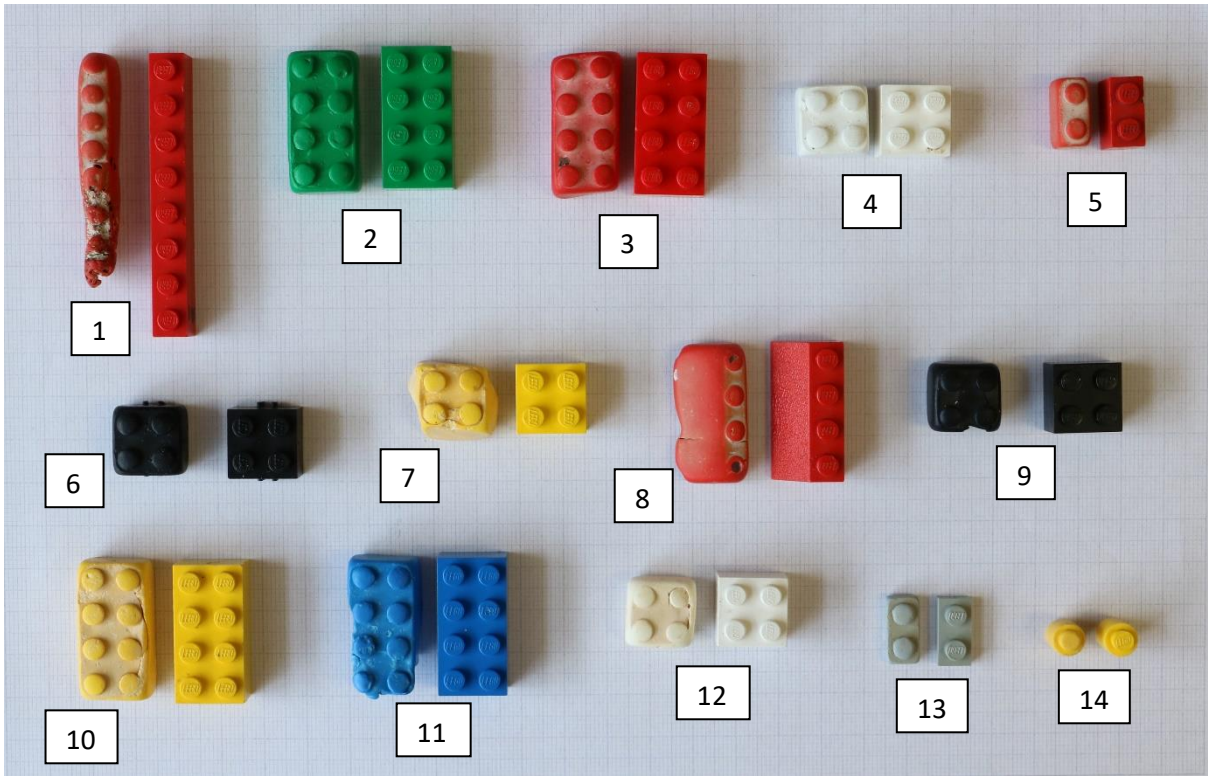
370

371

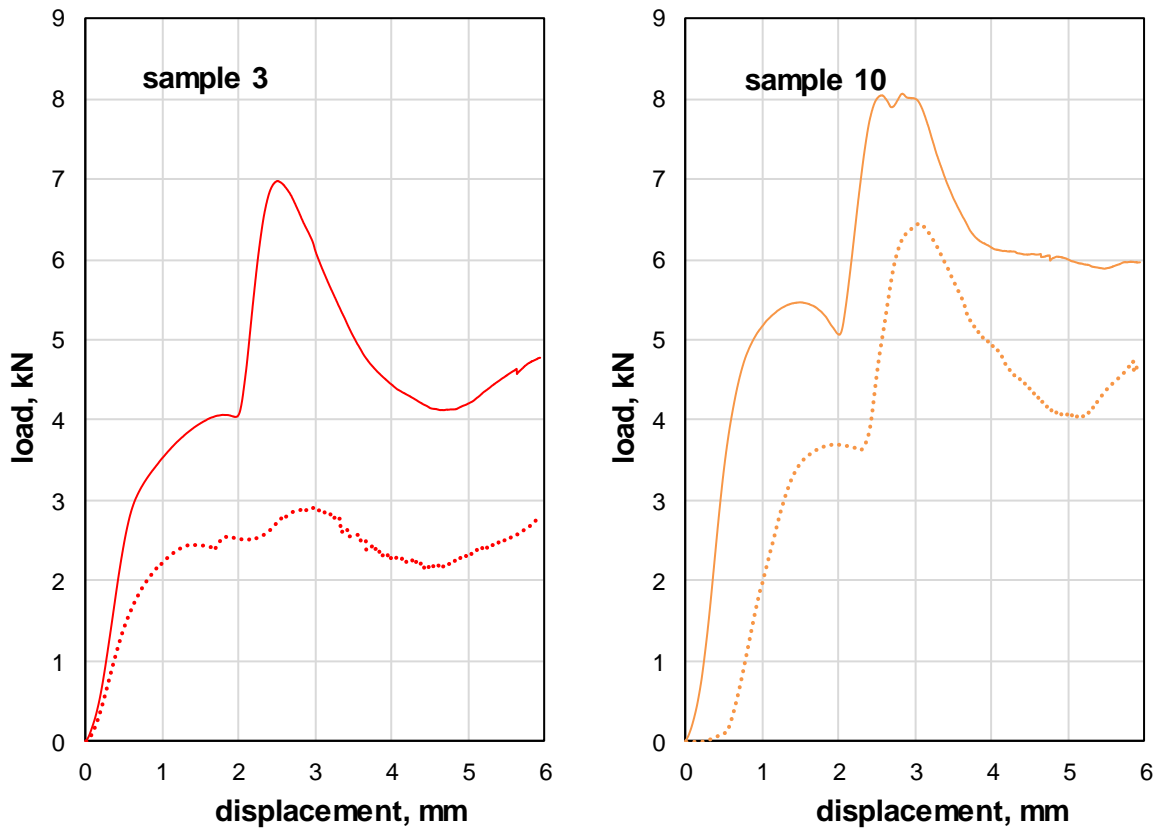
372

373

374



375 Figure 3: Load-displacement plots for unweathered blocks (solid lines) and weathered blocks (broken  
376 lines).



377

378

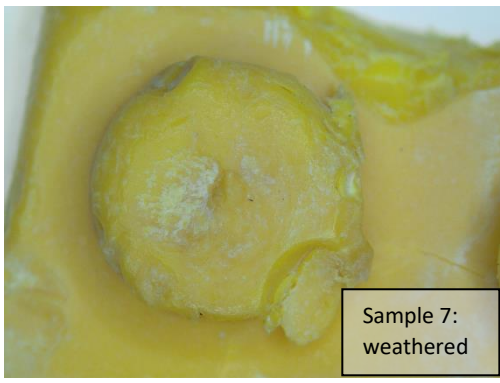
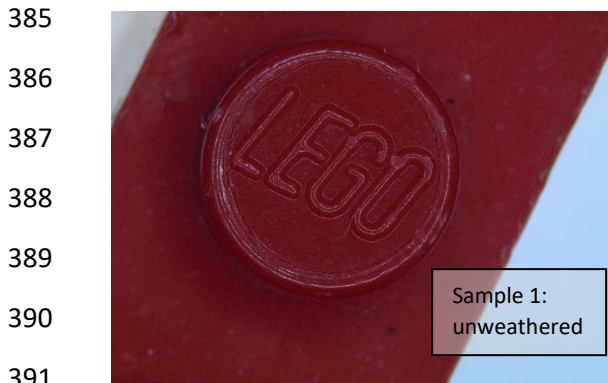
379

380

381

382

383 Figure 4: Microscopic images of sample pairs 1 and 7. For scale, the diameter of the studs on the left  
384 are 4.85 mm. Note the subtle change in font of the LEGO logo introduced in 1973.





393 Figure 5: Electron microscope images of the shorter exterior wall of an unweathered and weathered  
 394 LEGO block pair (sample 10) along with indicative elemental concentrations (in %) derived at the  
 395 locations shown circled in yellow. Note the presence of Cd as CdS in the unweathered block and the  
 396 presence of Ba as an additive only in the lighter regions; in the weathered block these elements are  
 397 absent at the surface because of the presence of residual salt and heterogeneous inorganic (e.g. Fe,  
 398 Al) and organic (e.g. Si) fouling.

399

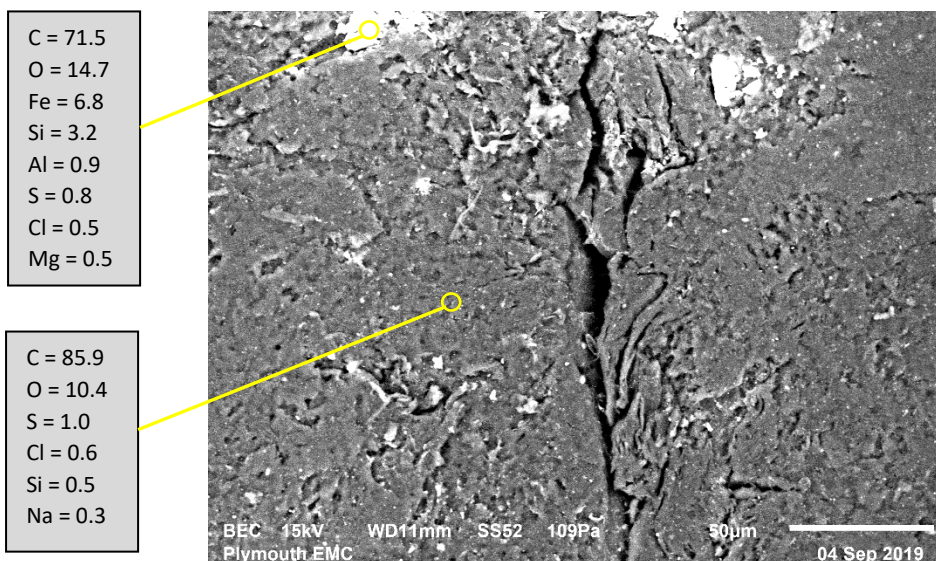
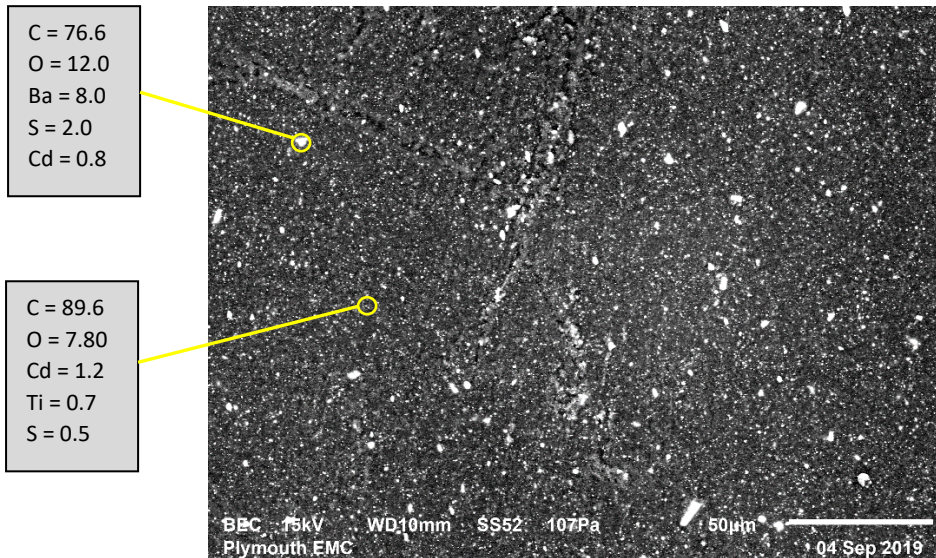
400

401

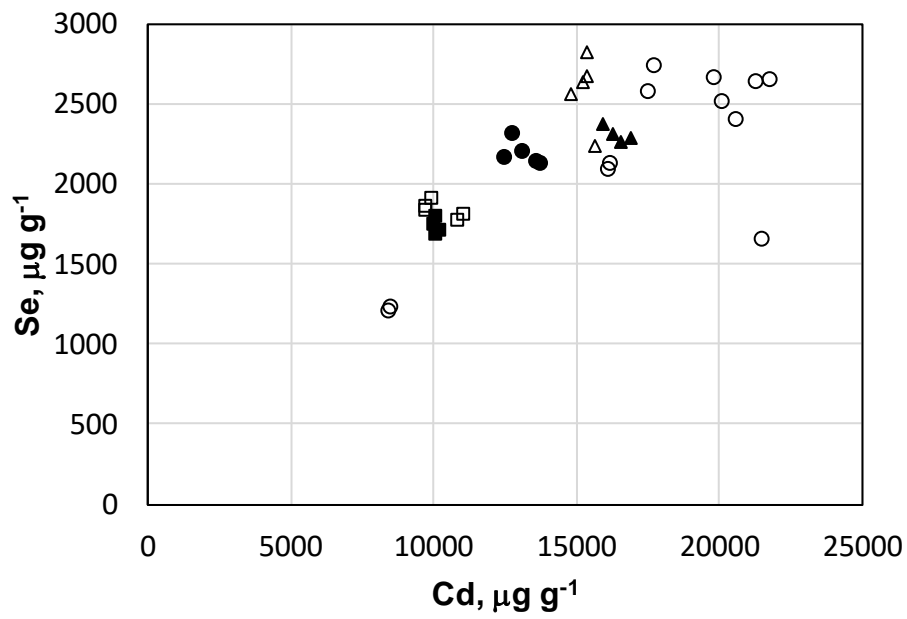
402

403

404



405 Figure 6: Concentrations of Se versus concentrations of Cd in three red samples pairs returned by  
 406 multiple XRF measurements of each block. Sample 1 = circles, sample 5 = triangles, sample 8 =  
 407 squares; filled symbols = unweathered blocks and open symbols = weathered blocks.



408  
 409  
 410  
 411  
 412  
 413  
 414  
 415  
 416  
 417  
 418  
 419  
 420  
 421  
 422  
 423  
 424  
 425

426 Figure 7: FTIR spectra between 700 and 4000  $\text{cm}^{-1}$  for (a) unweathered and (b) weathered blocks  
427 (sample 8 = red; sample 9 = black; sample 10 = yellow; sample 12 = blue). Note the accentuation of a  
428 peak at 1735  $\text{cm}^{-1}$  and the appearance of a peak at around 1270  $\text{cm}^{-1}$  in the weathered blocks.

